Оптический журнал

Оптическое приборостроение

A compact simultaneous full-Stokes vector polarimeter based on micro-retarder arrays

© 2018 B. X. Yao*, **, ***; PhD candidate; N. T. Gu*, **; Doctor; C. H. Rao*, **, Doctor

*The Key Laboratory on Adaptive Optics, Chinese Academy of Sciences, Chengdu, 610209, China
**Institute of Optics and Electronics, Chinese Academy of Sciences, Chengdu 610209, China
***University of Chinese Academy of Sciences, No.19A Yuquan Road, Beijing 100049, China

E-mail: chrao@ioe.ac.cn

Submitted 02.11.2017

The polarimeter is an important tool to measure polarization properties in the living human eye, to discriminate between benign and malignant moles, to measure solar magnetic field and so on. In this paper, we propose a new compact full-Stokes vector polarimeter to measure the full Stokes vector simultaneously which employ the micro-retarder arrays to replace the traditional moveable or adjustable wave-plate. Because of its compact structure, this polarimeter we propose can be used in different systems or different observation aims. And it also can be used in a large wavelength range. We have validated the feasibility of the proposed method by analytic and numeric ways, and the results show that we can get the full Stokes parameters simultaneously from one single image frame caught by this polarimeter.

Keywords: *polarimeter, simultaneous measure, micro-retarder arrays, imaging.*

OCIS codes: *350.1270, 120.5410, 120.0120, 230.3990.*

Компактный поляриметр с одновременным измерением всех компонентов вектора стокса, использующий матрицу миниатюрных линий задержки

© 2018 B. X. Yao; N. T. Gu; C. H. Raor

Поляриметры широко используются в офтальмологии, диагностике злокачественных опухолей, измерениях магнитных полей Солнца и т.п. Предложен новый компактный поляриметр, одновременно измеряющий четыре компонента вектора Стокса. Обычно используемые в конструкциях поляриметров сменные или переключаемые фазовые пластинки заменены на матрицу миниатюрных линий фазовой задержки. Поляриметр может проводить измерения в широком диапазоне длин волн и пригоден для разнообразных применений. Работоспособность предложенной схемы подтверждена численным моделированием и аналитически. Показано, что возможно одновременное получение полного набора компонентов вектора Стокса из единственного фрейма, полученного изображения на поляриметре.

Ключевые слова: *поляриметр, одновременные измерения, матрица линий фазовой задержки, обработка изображений.*

1. INTRODUCTION

Practically all solar phenomena are more or less relative to the solar magnetic field. It produces relatively stable structures like sunspots or prominences and is responsible for spectacular dynamic phenomena like flares or coronal mass ejections [1]. However, the generation, amplification and destruction of magnetic fields remain poorly understood. The knowledge of its magnitude and direction is crucial for interpreting measurements of other

parameters, and it can be measured usually by a polarimetry at some special spectral lines, which should be sensitive to the Zeeman effect. To answer what physical mechanisms are responsible for heating the corona, what causes variations of radiative output in the Sun, and what mechanisms trigger flares and coronal mass ejections and so on, many large aperture solar telescope have been developed (such as VTT [2], GREGOR [3], NST [4]) or have being developed (such as DKIST [5], EST [6]), and the Stokes polarimetry is their most important observational device for determining the magnetic field. New Solar Telescope (NST) employed a zero-order NIR wave plate as the polarimeter modulator, and two Wollaston prisms were adopted as the analyzers to offer a dual-beam to minimize seeing-induced spurious polarization [4]. Besides that, a Polarimetric Littrow Spectrograph (POLIS) was installed in the VTT for vector polarimetry, which includes a rotating modulator and two polarizing beam splitters in front of each CCD camera [7]. However, a movable wave plate both used in these two systems, cannot be modulated fast so that the observation data cannot be observed in real time. Besides that, movable optical components may introduce some measurement error, and some refractive optical elements will limit the usable spectral line. The Visible Imaging Polarimeter (VIP) is another kind of full vector polarimeter at VTT. It consists of two nematic Liquid Crystal Variable Retarders (LCVR) and a Wollaston prism [2]. This polarimeter based on LCVR is quite temperature sensitive, and its retardation must be calibrated frequently. Fast Solar Polarimeter (FSP) employed in GREGOR solar telescope used two Ferroelectric Liquid Crystals (FLC) instead of LCVRs to get a higher modulation frequency [8]. However the FLCs are useful just for only a limited wavelength range and it still cannot get the Stokes parameters in real time. To reduce the cross talk induced by bad seeing condition, the modulation and measurement should be as fast as possible, but these traditional systems cannot measure the polarimetric images in real time because of some movable components existing. Meanwhile, the stability and the measurement accurate will be limited by these movable parts. Moreover, the design and practical structure of these polarimeters is very different for different solar telescope or for different aims, and it is not very easy when we want to move the polarimeter from one telescope to the others. What's more, a four-detector photopolarimeter is proposed to measure the Stokes vector simultaneously [9]. But, it is not suitable for imaging polarimetry. To overcome the shortcomings mentioned above, we propose a polarimeter which can get the full Stokes parameters simultaneously from one single image frame. What′s more, this polarimeter is compact and integrated so it can be used on different systems and in a large wavelength range.

2. DEVICE DESIGN AND FABRICATION

In this letter, we proposed a new compact simultaneous full Stokes vector polarimeter, and it is illustrated in Fig. 1. It consists of a modulator and a camera, and the modulator includes two micro-retarder arrays with different fast axis and one polarizer. The each unit of these two micro-retarder arrays must be same size and be aligned with the pixels of CCD camera sensor, and the polarizer locates between the second array and CCD camera. We will introduce the basic principle of this method by a 2×2 units, and its schematic map is illustrated in Fig. 2.

After an incident light marked as $S = [I, Q, U, V]^{\mathrm{T}}$ passes through the polarimeter, the Stokes vector of the out light becomes $S' = [I', Q', U', V']^{\mathrm{T}}$ which comply with the following formula.

$$S' = M_{\mathrm{p}}(\theta_3) M_{\mathrm{r}}(\delta_2, \theta_2) M_{\mathrm{r}}(\delta_1, \theta_1) S, \qquad (1)$$

where $M_{\mathrm{p}(\theta)}$ is the Muller matrix of the polarizer, and $M_{\mathrm{r}(\delta,\theta)}$ is the Muller matrix of the retarder whose concrete expression are shown in (2) and (5).

$$M_{\mathrm{p}}(\theta) = R(-\theta) M_{\mathrm{p}}(0) R(\theta),$$

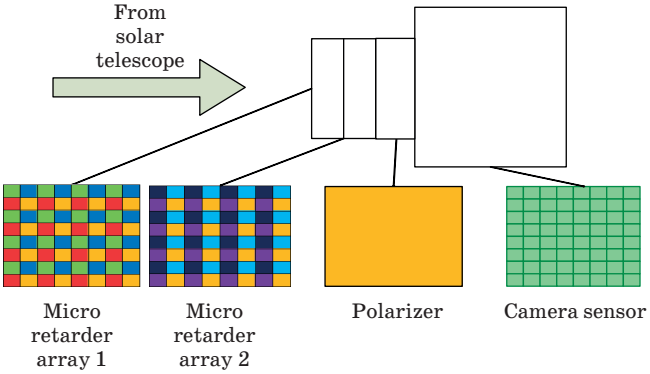

Fig. 1. Schematic diagram of the compact real-time full-Stokes vector camera. The camera sensor is placed on the focal plane of the solar telescope. The size of the micro-retarder units is same as the pixels.

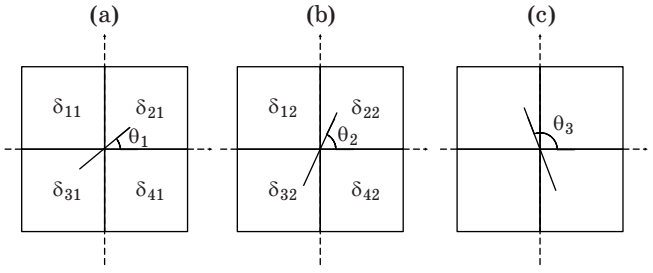

Fig. 2. Schematic diagram of the 2×2 units. (a) The 2×2 units of the first micro-retarder array have different retardation δ_{11}, δ_{21}, δ_{31}, δ_{41} and same orientation angle θ_1 of the fast axis. (b) The second array units have different retardation δ_{12}, δ_{22}, δ_{32}, δ_{42} and same orientation angle θ_2. (c) The orientation angle of the polarizer is θ_3.

$$M_{\mathrm{p}}(0)=0.5\begin{bmatrix}1&1&0&0\\1&1&0&0\\0&0&0&0\\0&0&0&0\end{bmatrix}, \tag{2}$$

$$R(\theta)=\begin{bmatrix}1&0&0&0\\0&\cos 2\theta&\sin 2\theta&0\\0&-\sin 2\theta&\cos 2\theta&0\\0&0&0&1\end{bmatrix}.$$

Here, $R(\theta)$ is the matrix of the coordinate conversion, and θ is the orientation angle of the polarizer.

$$R^{-1}(\theta)=R(-\theta). \tag{3}$$

$$R(\theta_1)R(\theta_2)=R(\theta_1+\theta_2). \tag{4}$$

$$M_{\mathrm{r}}(\delta,\theta)=R(-\theta)M(\delta)R(\theta),$$

$$M_{\mathrm{r}}(\delta)=\begin{bmatrix}1&0&0&0\\0&1&0&0\\0&0&\cos\delta&\sin\delta\\0&0&-\sin\delta&\cos\delta\end{bmatrix}. \tag{5}$$

Since the direction of the polarizer is fixed for this polarimeter, we can make this direction as the X axis of the reference coordinate system i.e. $\theta_3 = 0$. Therefore, equation (1) can be simplified as

$$\begin{aligned}S'=M_p(0)R(-\theta_2)M_r(\delta_2)\times\\ \times R(\theta_2)R(-\theta_1)M_r(\delta_1)R(\theta_1)S.\end{aligned} \tag{6}$$

To making the expression more simple, we let $S''=R(\theta_1)S$, $\alpha=-\theta_2$, and $\beta=\theta_2-\theta_1$. Then, equation (6) can be simplified further as shown below.

$$R(\theta_2)S'=M_p(\alpha)M_r(\delta_2)R(\beta)M_r(\delta_1)S''. \tag{7}$$

$$S=R(-\theta_1)S''. \tag{8}$$

As the camera can get the value of light intensities i.e. I' which expressed in (9) only, we ignore the expressions of the Q', U', and V'.

$$\begin{aligned}I'=0.5(a_1I+a_2Q+a_3U+a_4V),\\ a_1=1,\\ a_2=\cos 2\alpha\cos 2\beta-\sin 2\alpha\sin 2\beta\cos\delta_2,\\ a_3=(\cos 2\alpha\sin 2\beta+\sin 2\alpha\cos 2\beta\cos\delta_2)\cos\delta_1-\\ -\sin 2\alpha\sin\delta_2\sin\delta_1,\\ a_4=(\cos 2\alpha\sin 2\beta+\sin 2\alpha\cos 2\beta\cos\delta_2)\sin\delta_1+\\ +\sin 2\alpha\sin\delta_2\cos\delta_1.\end{aligned} \tag{9}$$

In the 2×2 micro-retarder units, without changing the directions, each retarder unit has different phase retardation. It means that light intensities got form these corresponding 2×2 pixels of the camera sensor correspond to four different modulation stations which form (10).

$$\begin{bmatrix}I_1'\\I_2'\\I_3'\\I_4'\end{bmatrix}=0.5\begin{bmatrix}a_{11}&a_{12}&a_{13}&a_{14}\\a_{21}&a_{22}&a_{23}&a_{24}\\a_{31}&a_{32}&a_{33}&a_{34}\\a_{41}&a_{42}&a_{43}&a_{44}\end{bmatrix}\begin{bmatrix}I''\\Q''\\U''\\V''\end{bmatrix},$$

$$\begin{aligned}a_{i1}=1,\\ a_{i2}=\cos 2\alpha\cos 2\beta-\sin 2\alpha\sin 2\beta\cos\delta_{i2},\\ a_{i3}=(\cos 2\alpha\sin 2\beta+\sin 2\alpha\cos 2\beta\cos\delta_{i2})\cos\delta_{i1}-\\ -\sin 2\alpha\sin\delta_{i2}\sin\delta_{i1},\\ a_{i4}=(\cos 2\alpha\sin 2\beta+\sin 2\alpha\cos 2\beta\cos\delta_{i2})\sin\delta_{i1}+\\ +\sin 2\alpha\sin\delta_{i2}\cos\delta_{i1}.\end{aligned} \tag{10}$$

Here δ_{i1} is the retardation of the first micro-retarder array, and δ_{i2} is of the second. The equation (10) can be simplified as

$$I=0.5AS''. \tag{11}$$

Only if the matrix A is invertible, i.e.

$$rank(A)=rank\left(\begin{bmatrix}a_{11}&a_{12}&a_{13}&a_{14}\\a_{21}&a_{22}&a_{23}&a_{24}\\a_{31}&a_{32}&a_{33}&a_{34}\\a_{41}&a_{42}&a_{43}&a_{44}\end{bmatrix}\right)=4. \tag{12}$$

the unique solution of Stokes vector S can be calculated from (13).

$$S=R(-\theta_1)S''=2R(-\theta_1)A^{-1}I. \tag{13}$$

We suppose the angle θ_1 equal to θ_2, i.e. $\beta = 0$, so the rank(A) = 3 because of $a_{12}=a_{22}=a_{32}=a_{42}=\cos 2\alpha$. We cannot get a unique or correct solution. Therefore, at least two micro-wave plate arrays with different fast axis orientation are needed for full-Stokes vector measurement. We have given a possible parameters according the requirement of rank(A) = 4, and it is listed in table. So we can get,

$$A=\begin{bmatrix}1&\sqrt{2}/2&-\sqrt{2}/2&0\\1&\sqrt{2}/2&\sqrt{2}/2&0\\1&0&0&-1\\1&0&0&1\end{bmatrix}.$$

And rank(A) = 4. It means the parameters listed in table are reasonable, and it can be used to measure the full-Stokes vector for some spectral lines.

Figure 3 shows the fabrication progress of the modulator. The retarder array units should be aligned to the camera pixels to reduce the cross talk between the neighbors. We illuminate the array with

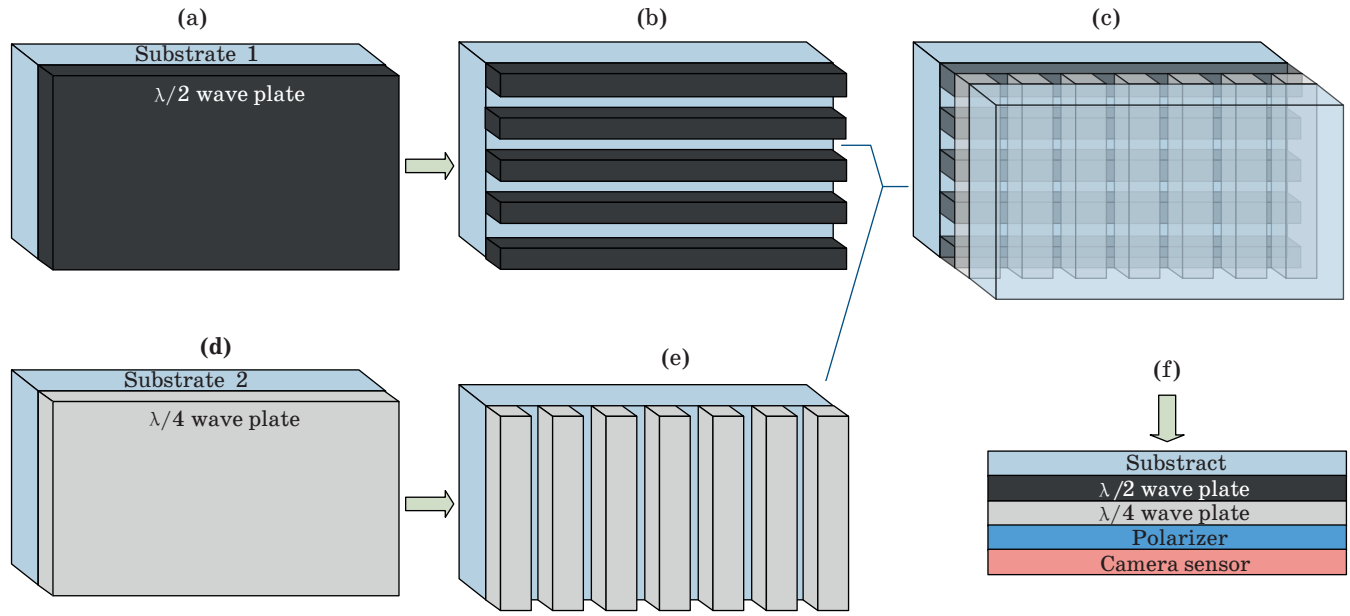

Fig. 3. Fabrication process of the polarimeter. (a) The λ/2 wave plate whose direction angle of the fast axis is 22.5° is pasted on the first substrate. (b) The wave plate is curved as a horizontal grating structure and the period is twice of the pixel size. (c) The direction angle of the λ/4 wave plate 45°. (d) The wave plate is curved as a longitudinal grating structure. (e) The λ/4 wave plate is pasted on the λ/2 one. (f) The second substrate is curved and the array is pasted on the camera sensor with a polarizer between them.

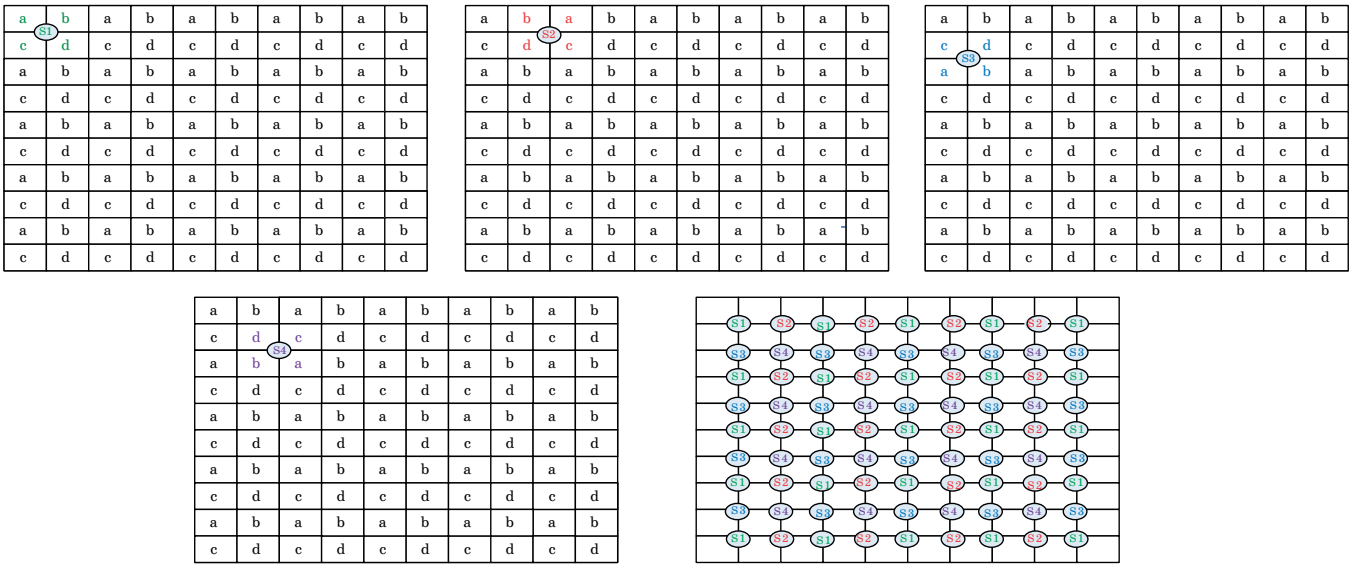

Fig. 4. The algorithm to improve the resolution. The 2×2 units with different colors correspond to different demodulation matrix.

a light through a polarizer in 0°, so its Stokes vector will be $S = [1\ -1\ 0\ 0]^T$ while pasting the array, and one of the intensities of the 2×2 units will be zero in theory. Then we adjust the retarder array until it is matched to the camera pixels.

The polarimeter we proposed use 2×2 pixels to demodulate the Stokes signal. It seems cannot make use of the full telescope resolution. So we improve the algorithm as shown in Fig. 4. The intensity of each pixel will be used in 4 different 2×2 units. So, if the number of the camera pixels is M×N, the resolution will reach to (M − 1)×(N − 1) and it will not decrease the resolution obviously.

3. CHARACTERIZATION OF THE POLARIMETER

The retardation of the wave plate based on birefringent crystals conforms to the formula (14). Where, δ is the retardation, d is the thickness of the crystal, and n_o, n_e are the refractive index corresponding

to the wavelength λ of the entered solar light. We can see that for specific wavelength λ and birefringent crystal, the retardation δ can be modulated by changing the thickness d of the crystal.

$$\delta(\lambda) = 2\pi / \lambda \left| n_{o(\lambda)} - n_{e(\lambda)} \right| d. \quad (14)$$

In this example, we use Calcite as the birefringent crystal which has good optical properties in a large range wavelength. And its performance is stable in both low and high temperatures. Here is its Sellmeier equation.

$$\begin{aligned} n^2_{o(\lambda)} &= 2.69705 + \\ &+ 0.0192064/(\lambda^2 - 0.01820) - 0.0151624\lambda^2, \\ n^2_{e(\lambda)} &= 2.18438 + \\ &+ 0.0087309/(\lambda^2 - 0.01018) - 0.0024411\lambda^2. \end{aligned} \quad (15)$$

Based on the spectral line of Fe I i.e. $\lambda = 0.6302$ μm and the retardation $\delta_1 = \lambda/2$ for the first wave plate, the thickness is calculated from (14) and (15) as $d_1 = 1.8493$ μm. And for the second, $d_2 = 0.9247$ μm. As soon as the structure of the polarimeter is conformed, for other spectral lines, we can get the retardation δ and then the modulation matrix A from (10) and (14) corresponding to their wavelength. As long as the rank(A) = 4, the equations (11) will have a unique and correct solution. It means this polarimeter can be used in a broad wavelength range.

For some reasons, there is always a detection error of the light intensities caught by the CCD camera marked as δI. And then the Stokes S″ calculated from (11) also has an error δS″ expressed on (16). However we always just care the relative error of the Stokes S″ which restricted by (17) without considering the error of the matrix A itself. Here $\| \ \|$ means the spectral norm of the vector or matrix. We suppose that the relative error of the light intensities caught by the CCD camera i.e. $\|\delta I\|/\|I\| = 10^{-4}$ (10). Then the relative error bound of the Stokes vector calculated from the formula (17) corresponding to the wavelength is shown in Fig. 5. If the request of $\|\delta S''\|/\|S''\|$ is 5×10^{-4}, then the polarimeter can be used to measure the full-Stokes vector in the wavelength range from 0.452 μm to 0.749 μm.

$$I + \delta I = 0.5A(S'' + \delta S''). \quad (16)$$

$$\|\delta S''\| / \|S''\| \le \|A\| \|A^{-1}\| \|\delta I\| / \|I\|. \quad (17)$$

4. NUMERICAL SIMULATIONS

To verify the correctness of the polarimeter, we have simulated the project using the software called Advanced System Analysis Program (ASAP), and Fig. 6 is the schematic map. Without considering a specific telescope system, we suppose the diameter of its exit pupil is 30 mm and its focal length is 1200 mm. So the F ratio of the solar telescope system is 40. The camera sensor which placed on the focal plane of the system has 512×512 pixels and the size of each pixel is 20 μm. We define the source array consist of 256×256 points with same light intensity and different polarization defined by Jones vectors corresponding to their place. And the wavelength are all 0.6303 μm. As mentioned before, we let the parameters of the modulator conform to the table. After a wave optics ray trace which let the beams coherent diffract, we get the distribution of the energy on the camera sensor plane. Then the full Stokes vectors are calculated with the method mentioned above.

The simulate result is shown in Fig. 7. We can learn that the difference of the Stokes parameters between the source and the calculation result is lower than 10^{-3}. The error is mainly caused by the oblique incidence of the light on the surface of the Calcite.

Parameters of the Polarimeter

Parameter 1	Value	Parameter 2	Value
δ_{11}	0	δ_{21}	0
δ_{12}	0	δ_{22}	90
δ_{13}	180	δ_{23}	0
δ_{14}	180	δ_{24}	90
θ_1	22.5	θ_2	45

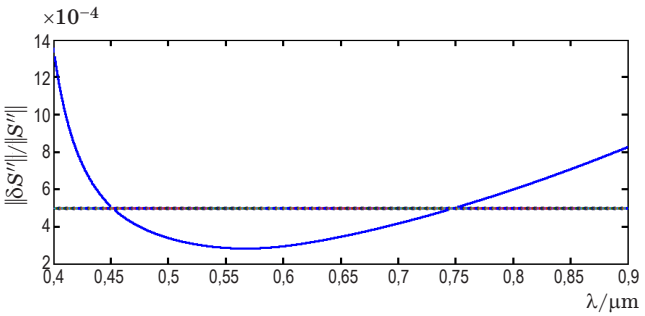

Fig. 5. The relative error bound of the Stokes vector i.e. $\|\delta S''\| / \|S''\|$ corresponding to the wavelength.

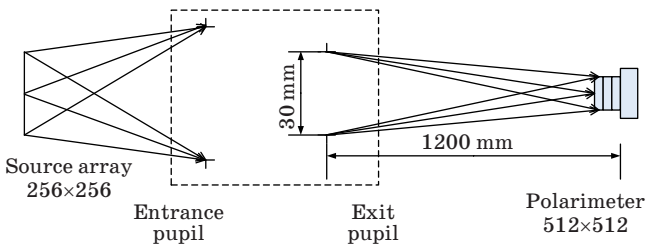

Fig. 6. The schematic map of the numerical simulation method.

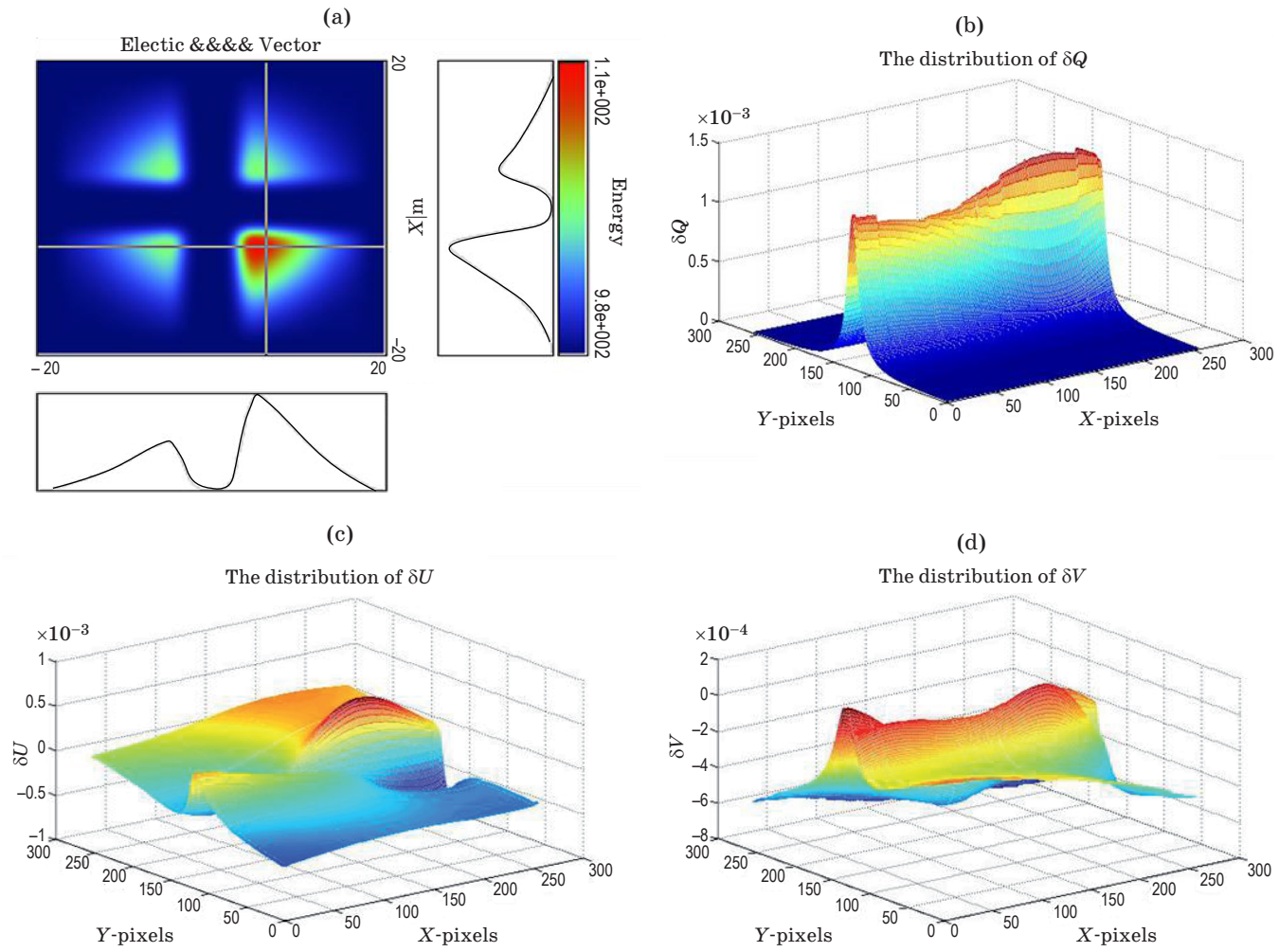

Fig. 7. (a) The distribution of the light intensities on 2×2 pixels unit. (b) The distribution of the error of the Q parameter calculated from the light intensities got by the camera. (c) The distribution of the error of the U parameter. (d) The distribution of the error of the V parameter.

However, as soon as the polarimeter fixed in the system, the matrix A will not change. So we can calibrate it in advance which means the error caused by oblique incidence does not influence the use of this polarimeter in a high accuracy system.

5. CONCLUSION

In conclusion, a new compact polarimeter is proposed to measure the solar Stokes vector simultaneously. A modulator, which includes two micro-retarder arrays and a polarizer are employed to replace the traditional moveable components and the stability and spectral range will be improved according our analysis. We have validated the feasibility of the proposed method, and a feasible example is also given. To verify the proposed method, we also simulated the polarimeter using the software ASAP. And the result conforms to our analysis. Only one image is needed to measure full-Stokes vector of input sunlight, and the influence of seeing-induced cross talk can be limited effectively. The proposed polarimeter can be used in different solar telescopes or different observation aims as soon as the F ratio of the system meet the requirement mentioned above. In current, we are trying to manufacture the proposed polarimeter, and more detailed reports will be introduced in next steps.

REFERENCES

1. *Hofmann A., Rendtel J.* Polarimetry with GREGOR // J. Proc. SPIE. 4843. Polarimetry in Astronomy. February 1, 2003. 112. doi: 10.1117/12.458615.

2. *Beck C., Bellot Rubio L.R., Kentischer T.J., Tritschler A., del Toro Iniesta J.C.* Two-dimensional solar spectropolarimetry with the KIS/IAA Visible Imaging Polarimeter // J. Astron. Astrophys. 2010. V. 520(17). P. 249–256.

3. *Von Der Lühe O., Schmidt W., Soltau D., Berkefeld T., Kneer F., Staude J.* GREGOR: a 1.5 m telescope for solar research // J. Astron. Nachr. 2001. V. 322(5–6). P. 353–360.

4. *Cao W., Ahn K., Goode P.R., Shumko S., Gorceix N., Coulter R.* The new solar telescope in Big Bear: Polarimetry II // ASP Conference Series 437. 2011. P. 345–349 .

5. *Keil S.L., Rimmele T.R., Oschmann J., Hubbard R., Warner M., Price R., Dalrymple N.* Science goals and development of the advanced technology solar telescope // J. Proceedings of the International Astronomical Union. 2004 (IAUS223). P. 581–588.

6. *Matthews S.A., Collados M., Mathioudakis M., Erdelyi R.* The European Solar Telescope (EST) // C. Proc. SPIE. Astronomical Telescopes + Instrumentation. 2016. P. 990809.

7. *Schmidt W., Beck C., Kentischer T., Elmore D., Lites B.* POLIS: A spectropolarimeter for the VTT and for GREGOR // J. Astron. Nachr. 2003. V. 324(4). P. 300–301.

8. *Iglesias F.A., Feller A., Nagaraju K., Solanki S.K.* High-resolution, high-sensitivity, ground-based solar spectropolarimetry with a new fast imaging polarimeter // J. Astron. Astrophys. 2016. V. 590. A89.

9. *Safronich I.N., Dorofeev D.L., Zon B.A.* Optimizing the parameters of a four-detector polarimeter // J. Opt. Technol. 2003. V. 70(3). P. 166–168.